Brain Anatomy

Introduction to Anthropogeny
Pascal Gagneux

Lecture 4
October 22, 2020

Levels of investigation

How do we study the composition of the brain non-invasively in humans & apes?

- Imaging of living brain (MRIs, DTIs, PET)
- Histology of brain after organ donation
- iPS cells

mRNA
RNA binding protein
miRNA

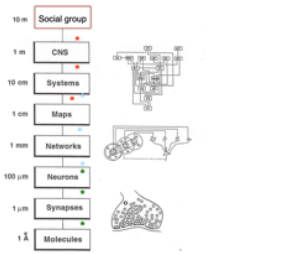

Sejnowski & Churchland 1992

Human Central nervous systems develop embedded in societies, cultural input is crucially important for neuro-typical development

---

The search for human-specific brain structures

Owen-Huxley Debate

R. Owen (Wikipedia. Com)

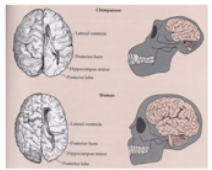

Thomas Henry Huxley (1825-1895) – "Darwin's Bulldog"

(Caricature of Huxley by Carlo Pellegrini in Vanity Fair 1871)

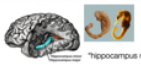

"hippocampus minor" now calcar avis

Claims for uniquely human brain features have a long tradition, but require rigorous comparisons.

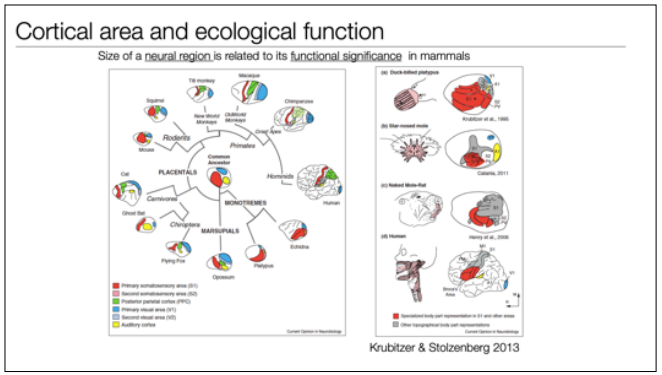

The mammalian cortex can devote different amounts of real estate to particularly relevant features.

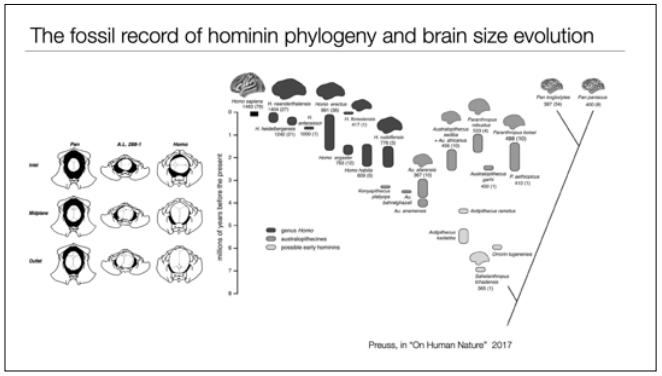

The fossil record of hominin phylogeny and brain size evolution. Date ranges for fossils are from Wood and Baker (2011). Brain sizes (incubic centimeters) are from de Sousa and Cunha (2012) and, for Pan paniscus only, from Hopkins et al. (2009). Sample sizes are indicated in parentheses. Wood and Baker are not explicit about the details of relationships among each of the species, but there is general agreement that the genus Homo evolved from an australopithecine ancestor.

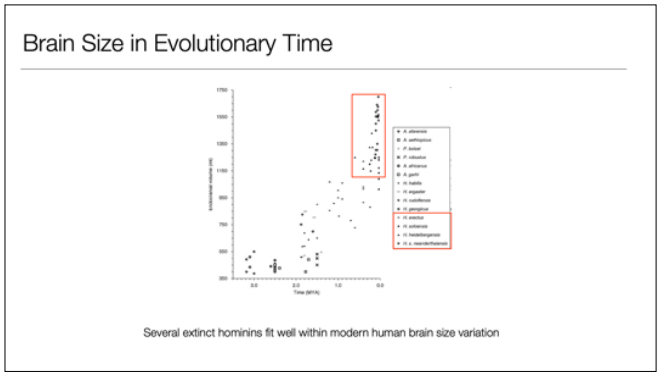

Absolute Brain Size

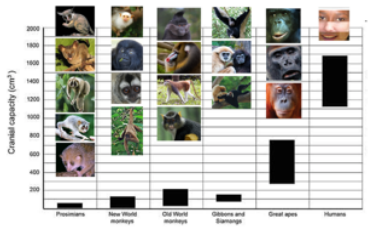

Humans have the largest brain size among primates

D. Falk, 1986

How to grow a big brain

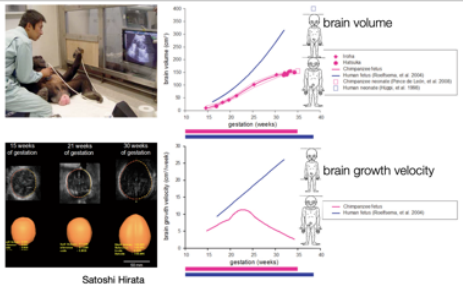

Satoshi Hirata

Sakai et al. **Current Biology**, 2012

Gestational age-related changes in brain volume in chimpanzee (Hatsuka and Iroha) and human fetuses.
Gestational age-related changes in the growth velocity of brain volume in chimpanzee and human fetuses
Chimpanzee brains start slowing down their growth in mid-pregnancy, humans on the other hand continue a high fetal rate for a full year after birth.

Brain development: from tube to walnut

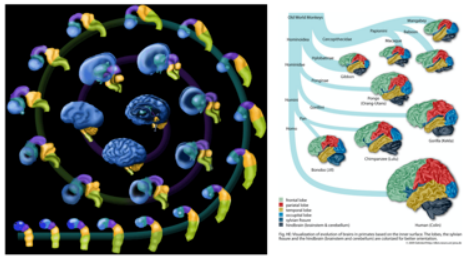

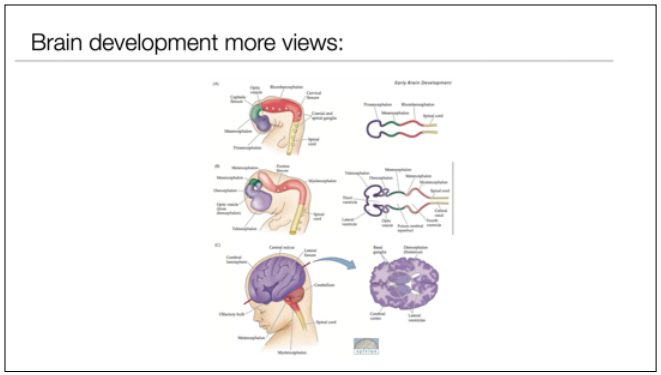

Much of the hollow space under the cortex (with a thickness of 1 to 7mm, average in humans 2.5mm) becomes filled with connections (white matter)

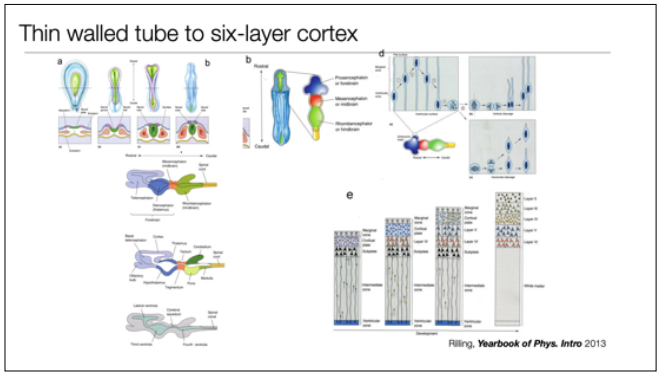

Mechanisms of neurodevelopment. (a) Formation of the neural tube, (b) development of forebrain, midbrain, and hindbrain
vesicles, (c) development of major CNS divisions, (d) neurogenesis, (e) neuronal migration. [Reprinted from Bear MF et al.2001. Neuroscience: Exploring the Brain. Pages 179–711. C 2001

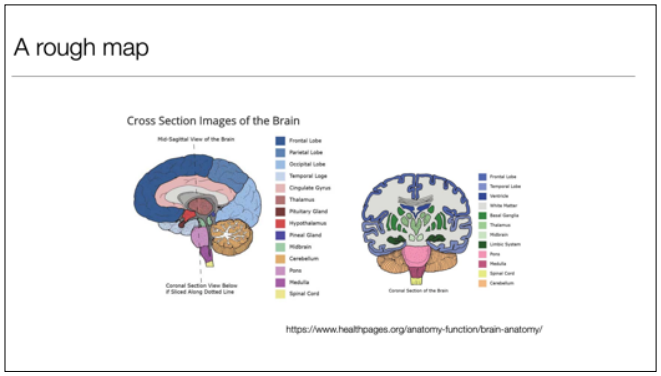

Anatomist have coined distinct names for distinct regions of the cortex and subcortical regions of the brain.

Cortical thickness and variation

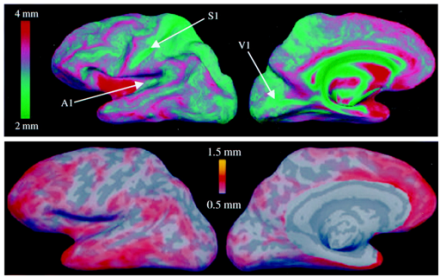

Fishl & Dale, Measuring the thickness of the human cerebral cortex from magnetic resonance images. 2000. ***PNAS***

Overview of the human central nervous system

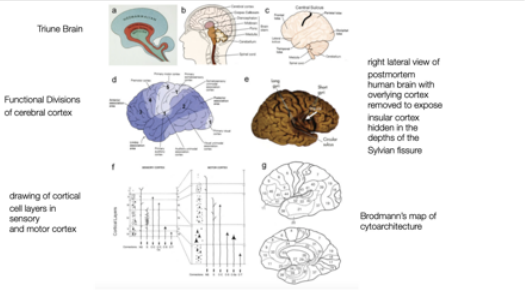

Rilling, Yearbook of Phys. Intro 2013

Overview of the human central nervous system.
(a) Triune brain model, (b) seven main divisions of central nervous system, (c) lateral view of the
human brain, (d) functional divisions of cerebral cortex, 1 5 primary sensory and motor
cortex, 2 5 association
cortex, 3 5 prefrontal cortex, 4 5 premotor cortex, 5 5 primary motor cortex, (e) right lateral view of postmortem human brain with
overlying cortex removed to expose insular cortex hidden in the depths of the Sylvian fissure, (f) drawing of cortical cell layers in sensory
and motor cortex, (g) Brodmann's cytoarchitectonic map of the human cerebral cortex, (h) the limbic system, (i) the mesolimbic dopamine system, (j) drawing of neuron, (k) synaptic transmission.

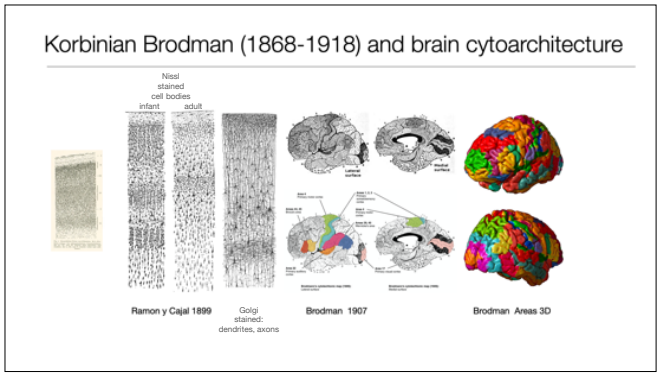

Nissl-stained visual cortex of a human adult. Middle: Nissl-stained motor cortex of a human adult. Right: Golgi-stained cortex of a 11⁄2 month old infant. The Nissl stain shows the cell bodies of neurons; the Golgi stain shows the dendrites and axons of a random subset of neurons.

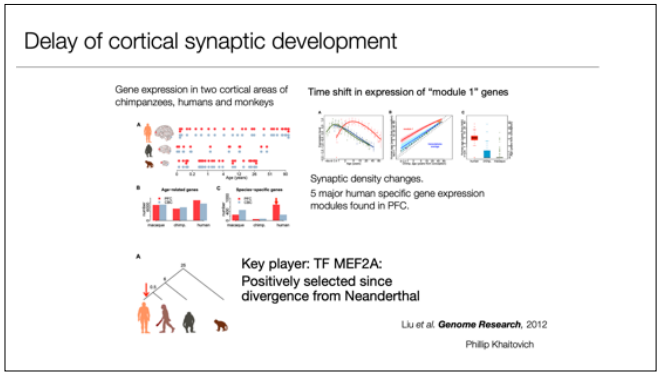

Age-related gene expression change in the PFC and CBC. (A) Age distribution of samples used in this study. Each point represents an individual, with technical replicates shown as a second point below the first. Only one of the two replicates was used in the main analysis. Thecolors indicate brain regions (red, PFC; gray, CBC). The x-axis representsindividual age in fourth root (age1/4) scale. Numbers of age-related genes(B) and genes with species-specific expression profiles (C) identified in the PFC (red) or CBC (gray). The red arrows highlight excess human-specific expression changes in the PFC.

Synaptic density changes during human, chimpanzee, and macaque PFC development. (A) Example of synapses viewed by electron microscopy (red arrows), in the PFC of a 32-d-old chimpanzee. (B)Mean synaptic density per 100 mm2 measured in the PFC of humans (red), chimpanzees (blue), and rhesus macaques (green) at different ages. (Error bars) 95% confidence intervals obtained by bootstrapping synaptic density values within samples 1000 times. Independent assessment of synaptic density by another investigator is plotted on Supplemental The phylogenetic relationship of human, Neanderthal, chimpanzee, and rhesus macaque species. (Red arrow) Human lineage. The numbers show approximate divergence time in millions of years (Kumar and Hedges 1998; Pa¨a¨bo 1999; Chen and Li 2001). (B)

Proportion of human-derived SNPs measured using a 50-kb slidingwindow in the MEF2A gene region (red). SNPs were classified as derived according to the method described by Green et al. (2010). (Gray dashed line) Genome average. (Red arrow) Location, upstream of MEF2A, with significant excess of human-derived SNPs (one-sided Fisher's exact test, P = 0.00006). (C) Distribution of the proportion of human-derived SNPs for all windows across the human

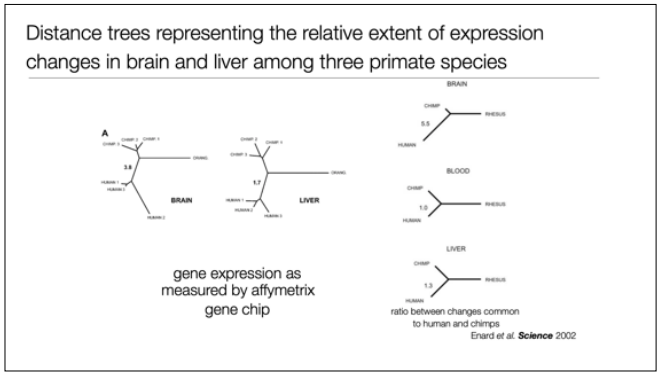

Distance trees representing the relative extent of expression changes in brain and liver among three primate species. Individual humans can have gene expression differences in the cortex that are almost as large as that between a human and a chimpanzee!

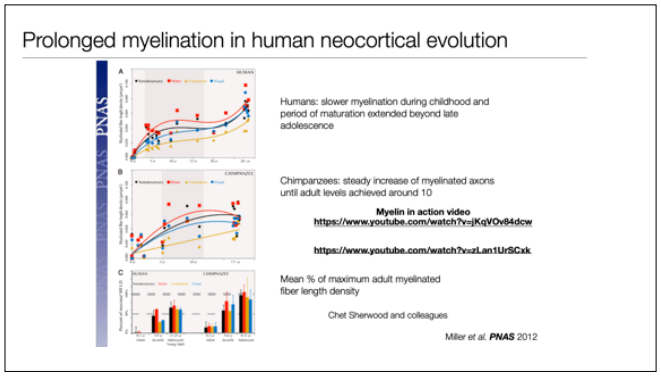

Developmental trajectory of myelinated fiber length density (MFLD). Graphs show best-fit curves for MFLD data in humans (A;n=24) and chimpanzees (B;n=20) arranged by age in years. The shaded vertical area represents time between weaning and full sexual maturation. Diamonds represent somatosensory area (area 3b), squares represent motor area (area 4), triangles represent frontopolar area (area 10), and circles represent visual area (area 18). (C) Bar graph depicts mean percent of maximum mature adult MFLD across development in humans (Left) and chimpanzees (Right). Error bars represent SEM. The thin and thick horizontal dashed lines represent 50% and 100%, respectively, of maximum MFLD. Black represents

somatosensory area (area 3b), red represents motor area (area 4), goldrepresents frontopolar area (area 10), and blue represents visual area (area 18).

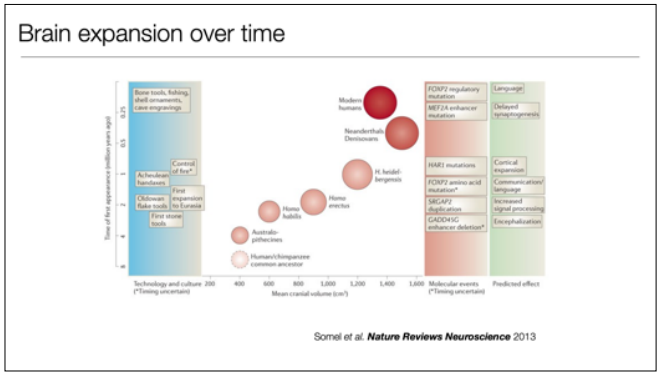

Anatomical differences between human and chimpanzee brains, changes in cranial size in the human fossil record, and archaeological records of tools and cultural artefacts together present a general picture of the evolutionary steps that have led to the emergence of the human brain and cognitive abilities. From the most recent common ancestor of humans and chimpanzees 6–8 million years ago (mya) until the dawn of the genus Homo approximately 2.5 mya, all early human ancestors had ape-like cranial volumes. By contrast, subsequent Homo species had both higher absolute cranial capacities and higher cranium-to-body ratios (also known as encephalization quotients). For example, the early Homo habilis (2.3–1.6 mya) had a cranium that was 1.5 times larger than that of modern chimpanzees. Homo erectus, a hominid species that populated our planet between 1.9 mya and 200 thousand years ago (kya), had a cranium that was initially twice as large. Homo heidelbergensis, another hominin ancestor that appeared approximately 1 mya, had a cranial capacity approximately three times that of modern chimpanzees, overlapping with that of modern humans (Homo sapiens sapiens, 200 kya149), whereas Neanderthals (Homo sapiens neanderthalis, from 400–800 kya to 30 kya35, 39) evolved cranial sizes that surpassed those of modern humans. Compared to ancestral hominins, increased cranial capacity probably augmented the general and social

intelligence of Homo species. Encephalization might have been the basis for the Oldowan (2.6–1.4 mya) and Acheulean (1.8–0.25 mya) stone tool technologies, and could have set the ground for the first out-of-Africa hominin colonizations undertaken by Homo erectus. Tool use for scavenging, hunting and digging tubers, and the subsequent control of fire and invention of cooking are thought to have promoted human encephalization by enriching nutritional content and increasing energy input. Technological advance, access to high-quality food and encephalization thus appear to have evolved hand-in-hand. However, exceptions to this concept of parallel evolution might exist, such as the not yet fully understood case of the small-brained Homo floresiensis species, who used stone tools but had an ape-like cranial volume.

Recent comparative genomic studies have identified a number of mutations in the modern human genome that could underlie the evolution of larger brain size and behavioural traits. In agreement with the fossil record, these mutations are shared with extinct hominin species, indicating that encephalization and certain behavioural changes evolved early in the evolution of Homo. For example, a deletion of one enhancer of the growth arrest and DNA-damage-inducible gamma (GADD45G) gene, which is postulated to have led to brain size expansion, is shared with Neanderthals). Likewise, a human-specific duplication of a truncated version of the gene SLIT-ROBO Rho GTPase activating protein 2 (SRGAP2) was dated to approximately 2.4 mya. This duplication is predicted to increase dendritic spine density in the cortex and could have enhanced signal processing in the hominin brains (see the figure). It is also worth noting that both Neanderthals and Denisovans — the two extinct hominin species that diverged from the human evolutionary lineage 400–800 kya differ from other primates by the same two amino acid changes as modern humans in the gene encoding forkhead box P2 (FOXP2). As these amino acid substitutions have been linked to the evolution of human language and changes in brain connectivity, it is conceivable that Neanderthals and Denisovans also possessed certain

types of human-like linguistic abilities.Remarkably, although the late Homo species showed an increase in brain size to and beyond that of modern humans, their Acheulean technology (1.8–0.25 mya), mainly consisting of stone flakes and hand-axes, made only limited progress for nearly 1.5 million years. This cultural and technological standstill contrasts with the rapid cultural explosion observed in the archaeological record that started approximately 250 kya and is associated with the appearance of the first fossil remains of modern humans, Homo sapiens sapiens. The first modern human forms appear about 190 kya in East Africa, which is in agreement with the estimation for the origin of modern humans based on population genetic studies. With the rise of modern humans in Africa, between 250 and 50 kya, bone tools began to be exploited, and spear heads and fishing appeared. Besides technological innovation, this period also witnessed the first appearance of unequivocal symbolic artefacts, such as pigment use by 160 kya and shell ornaments and cave engravings by 77 kya. Producing these artefacts involved a large number of steps, and maintaining such a culture demanded efficient systems of information transfer across generations5. This cultural explosion was soon followed by successful colonization of other continents and could have accelerated the extinction of other hominin species. Strikingly, the now-extinct hominins that coexisted with Homo sapiens — including Neanderthals — do not appear to have produced symbolic artefacts, despite Neanderthals having a larger cranial capacity than Homo sapiens.

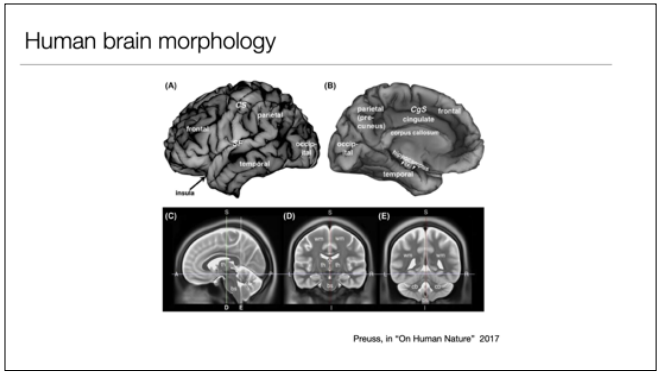

Human brain morphology. (A, B) The location of the major lobes are shown in lateral (A) and medial (B) views of the left cerebral hemisphere. The central sulcus (CS) separates the frontal and parietal lobes; the Sylvian fissure (SF) separates the temporal lobe from the frontal and parietal lobes. The insula is a region of limbic cortex buried within the SF. The cingulate sulcus (CgS) separates the cingulate cortex from the frontal and parietal cortex. (CeE) T2-weighted MRI images showing the relationship of the cerebral hemispheres to deep structures, including the thalamus (th), cerebellum (cb), and brainstem (bs). The section in C is in a parasagittal plane, with anterior (A) to the left. D and E are coronal sections; their locations are marked in C. In T2-weighted images, the cortical gray matter appears as a light rim surrounding the darker white matter (wm). Images were captured from the Human Connectome Project (HCP) datasets using HCP Workbench software. Additional abbreviations: I, inferior; L, left; P, posterior; R, right.

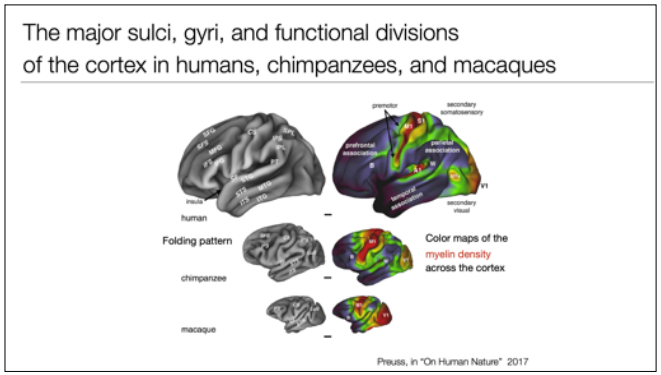

Laminar, columnar, and areal organization of cerebral cortex. (A) An unstained section through the posterior right cerebral hemisphere of a human; the inset shows the small region of gray matter illustrated at higher magnification in B. (B) A section of cortical gray matter stained for Nissl substance to illustrate the six tangential layers and the vertically oriented mini-columns. In this section, the columnar appearance of the cortex is most obvious in layers 4 and 5. (C) A schematic representation of cortical microstructure, showing the vertical clustering of neurons and the predominantly vertical, intracolumnar organization of intrinsic (local) connections, although some layers also have prominent horizontal, intralaminar connections as well. Most long

connections travel in the white matter (wm). Collections of continuous minicolumns, with similar connections and cellular organization, make up the areas, the next higher-order unit. (D, E) Low-magnification view of a horizontal section through the posterior right hemisphere of an orangutan, stained for Nissl (D) and myelin (E) to illustrate cyto- and myeloarchitectonic differences between cortical areas. Posterior is to the left, lateral to the bottom. In both stains, the distinctive, highly laminated character of the primary visual area (V1) is apparent, and the border between V1 and the second visual area (V2), marked with arrowheads, is easily identified. Laterally, the border is close to the lip of the lunate sulcus (LuS, a deep fissure in apes and macaques, but absent in monkeys). While the other cortex in these sections is not homogeneous in Nissl or myelin, distinct borders, such as that between V2 and V3, which presumably occupies the anterior bank of the LuS, are often difficult to distinguish.

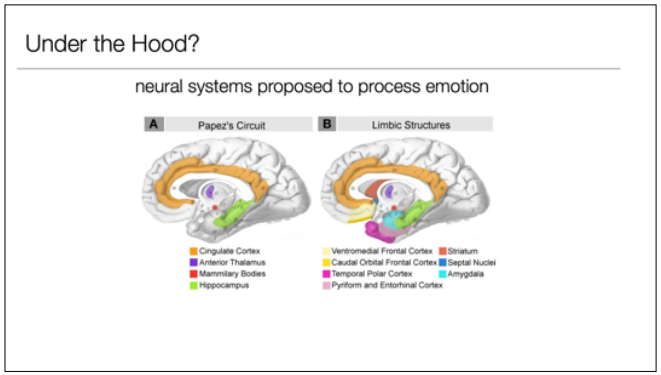

Schematic briefly summarizing neural systems proposed to process emotion, highlighting structures that are visible on the medial surface of the brain. Papez's(1937) original circuit (A) was expanded upon in the concept of the limbicsystem (B) to include a variety of subcortical and cortical territories (MacLean, 1952; Heimer and VanHoesen, 2006). (Structures like the anterior insula and nucleus basalis of Meynert, which are not visible on the medial surface of the brain ,are not represented here). Images modifiedfrom Papez's(1937) original drawing.

Subcortical brain structures

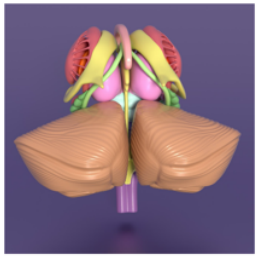

https://www.turbosquid.com/3d-models/3d-obj-realistic-subcortical-structures-human-brain/818190

Subcortical brain structures

https://www.turbosquid.com/3d-models/3d-obj-realistic-subcortical-structures-human-brain/818190

Subcortical brain structures

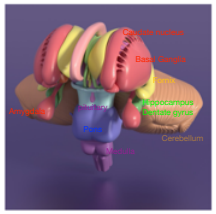

https://www.turbosquid.com/3d-models/3d-obj-realistic-subcortical-structures-human-brain/818190

Relative Size of Frontal Cortex

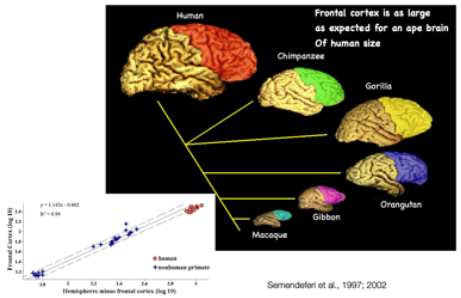

Semendeferi et al., 1997; 2002

Anatomically informed boundaries show that..

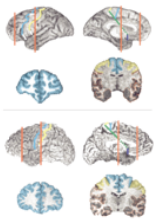

The human frontal cortex, both
a) with and b) without
the precentral gyrus (primary
motor cortex) is as large
as expected for an ape of human
brain size

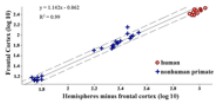

Semendeferi et al., 1997; 2002

Radial unit lineage model of cortical neurogenesis

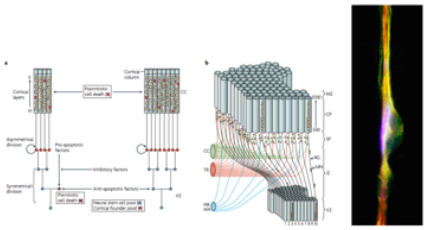

Rakic, P 2009 ***Nature Rev Neurosciences***

Radial unit lineage model of cortical neurogenesis. a | Based on the radial unit hypothesis12,30, the model illustrates how changes in the mode and the rates of cell proliferation and/or programmed cell death within the neural stem cell pool (blue circles) in the ventricular zone (VZ) that divide symmetrically at early embryonic stages causes an exponential increase in the number of radial columns, which, in turn, results in surface expansion of the cerebral cortex without changes in its thickness. By contrast, similar changes in proliferation kinetics occurring in the founder cells (red circles), which divide asymmetrically, cause a linear increase in the number of neurons within radial columns without a change in the cortical surface area. b

| The model of radial neuronal migration that underlies columnar organization. The cohorts of neurons generated in the VZ traverse the intermediate zone (IZ) and subplate zone (SP) containing ‘waiting’ afferents from several sources (cortico-cortical connections (CC), thalamic radiation (TR), nucleus basalis (NB), monoamine subcortical centers (MA)) and finally pass through the earlier generated deep layers before settling in at the interface between the cortical plate (CP) and marginal zone (MZ). The timing of neurogenesis (E40–E100) refers to the embryonic age in the macaque monkey. The positional information of the neurons in the VZ and corresponding protomap within the SP and CP is preserved during cortical expansion by transient radial glial scaffolding. Further details can be viewed in the Rakic laboratory animated video of radial migration. RG, radial glia cell; MN, migrating neuron.

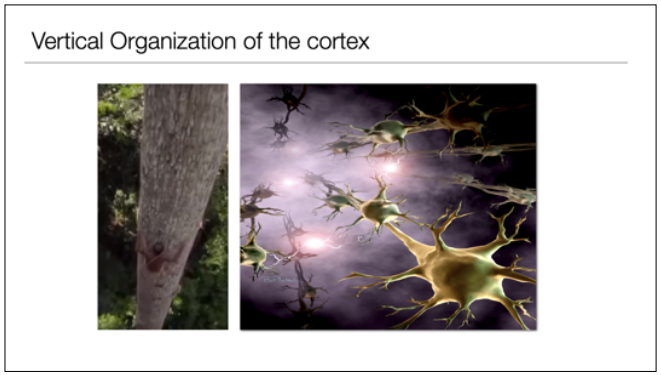

Like a pygmy man climbing a giant tree to find honey, neurons from the subventricular zone climb along dial glial cells during cortical development.

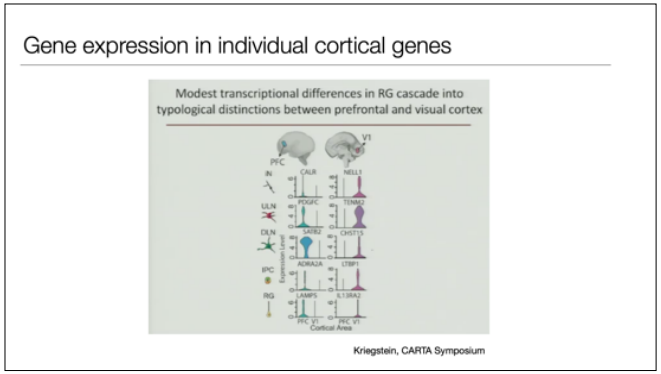

Kriegstein, CARTA Symposium
Gene expression in radial glia can differ depending on region of the brain. Radial glia cells disappear once the cortex is established!

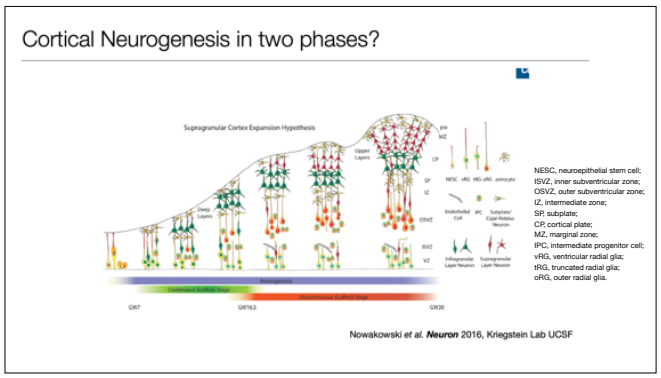

Nowakowski et al. Neuron 2016, Kriegstein Lab UCSF
The Supragranular Cortex Expansion Hypothesis: By integrating experimental evidence in the published literature with our experimental findings, we propose that primate cortical neurogenesis can be divided into two stages. During early neurogenesis (left), basal fibers of ventricular radial glia contact the pial surface and newborn neurons migrate along ventricular as well as outer radial glia fibers. During late neurogenesis (right), newborn neurons reach the cortical plate only along outer radial glia fibers. VZ, ventricular zone; NESC, neuroepithelial stem cell; ISVZ, inner subventricular zone; OSVZ, outer subventricular zone; IZ, intermediate zone; SP, subplate; CP, cortical plate; MZ, marginal zone; IPC, intermediate progenitor cell; vRG, ventricular radial glia; tRG, truncated radial glia; oRG, outer radial glia.

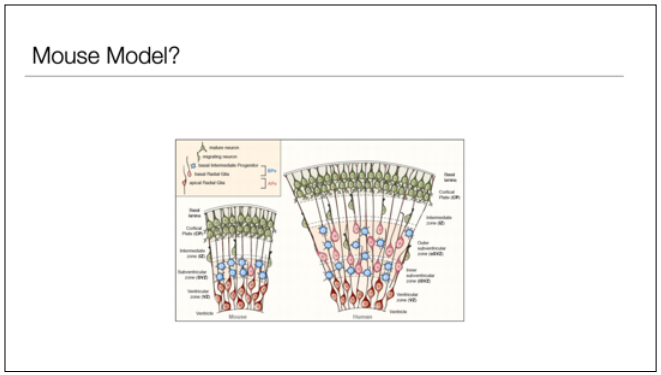

Cartoon illustrating APs and BPs in embryonic mouse and fetal human neocortex. Mouse is left, human is right. Note the increase in BPs and the expansion of the SVZ in fetal human neocortex.

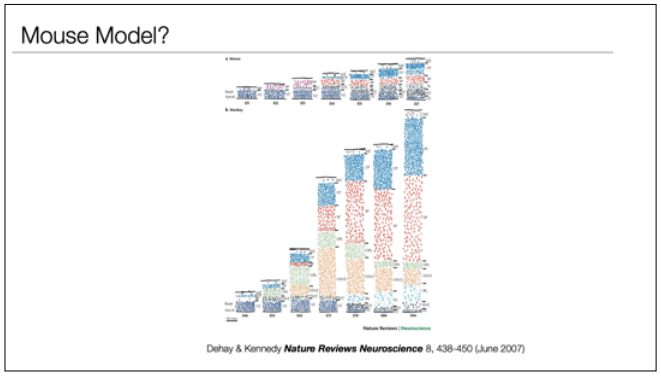

Dramatic differences in size and cellular architecture between mouse and human cortex.

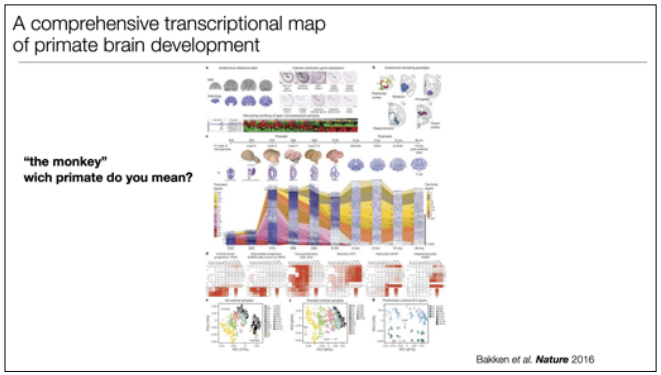

The transcriptional underpinnings of brain development remain poorly understood, particularly in humans and closely related non-human primates. We describe a high-resolution transcriptional atlas of rhesus monkey (Macaca mulatta) brain development that combines dense temporal sampling of prenatal and postnatal periods with fine anatomical division of cortical and subcortical regions associated with human neuropsychiatric disease. Gene expression changes more rapidly before birth, both in progenitor cells and maturing neurons. Cortical layers and areas acquire adult-like molecular profiles surprisingly late in postnatal development. Disparate cell populations exhibit distinct developmental timing of gene expression, but also

unexpected synchrony of processes underlying neural circuit construction including cell projection and adhesion. Candidate risk genes for neurodevelopmental disorders including primary microcephaly, autism spectrum disorder, intellectual disability, and schizophrenia show disease-specific spatiotemporal enrichment within developing neocortex. Human developmental expression trajectories are more similar to monkey than rodent, although approximately 9% of genes show human-specific regulation with evidence for prolonged maturation or neoteny compared to monkey.

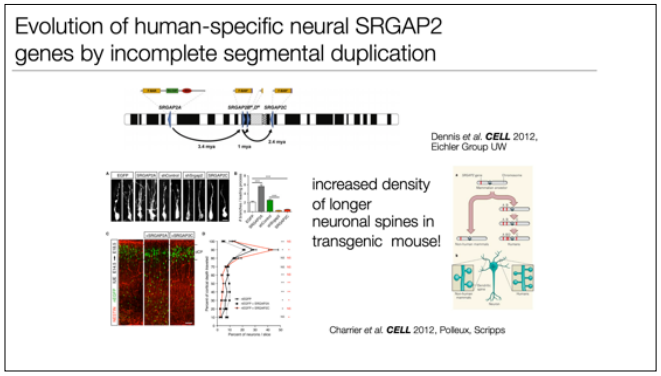

SLIT-ROBO Rho GTPase-activating protein 2 (srGAP2) also known as formin-binding protein 2 (FNBP2) is a protein that in humans is encoded by the SRGAP2 Schematic depicts location and orientation (blue triangles) of SRGAP2 paralogs on human chromosome 1 with putative protein products indicated above each based on cDNA sequencing. Asterisks indicate a 49 amino acid truncation of the F- BAR domain. Note that the orientation ofSRGAP2D remains uncertain, as the contig containing this paralog has not yet been anchored. Arrows trace the evolutionary history of SRGAP2duplication events. Copy number polymorphism and expression analyses suggest both paralogs at 1q21.1 (SRGAP2B and SRGAP2D) are pseudogenes, whereas the 1q32.1 (SRGAP2A) and 1p12 (SRGAP2C) paralogs are likely to encode functional proteins.
SRGAP2C Expression in Radially Migrating Mouse Cortical Neurons Phenocopies Srgap2 Knockdown (A) Confocal images of optically isolated neurons showing representative morphologies of radially migrating cortical neurons in E18.5 embryos following in utero electroporation (IUE) at E14.5 of the indicated constructs. sh, short hairpin. Scale bar, 10 mm. (B) Mean number of branches (±SEM) of the leading process of neurons as represented in (A). n = 3 animals/condition, 100–150 neurons/condition. (C) Low magnification confocal images of E18.5 cortical slices showing

migration of in utero electroporated neurons expressing nuclear-EGFP (nEGFP) alone or together with SRGAP2A or SRGAP2C. Staining with anti-GFP shows the position of the electroporated neurons, and anti-NESTIN marks the radial glial scaffold. dCP, dense Cortical Plate.(D) Quantification of neuron distribution in cortical slices as illustrated in (C) (mean ±SEM). n = 3 animals/condition, 9–10 slices/condition. In (B) and (D), *p < 0.05; **p < 0.01; ***p < 0.001; NS (not significant, p > 0.05); Mann-Whitney test.

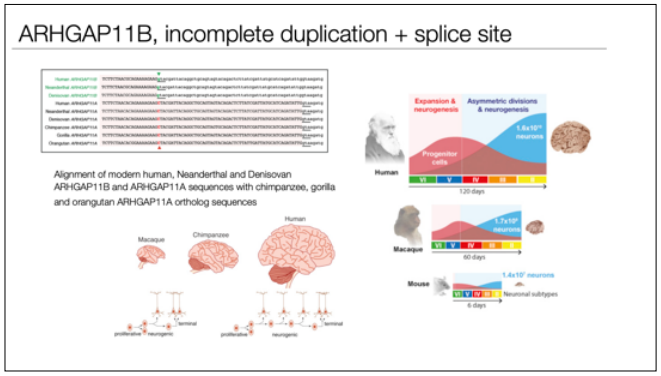

Reconstruction of the ancestral splice donor site. Alignment of modern human, Neanderthal and Denisovan ARHGAP11B and ARHGAP11A sequences with chimpanzee, gorilla and orangutan ARHGAP11A ortholog sequences. The boundaries between exons 5 (pink rectangles) and introns 5 are shown. Arrowheads indicate the C- to-G nucleotide substitution (red-to-green) in exons 5. Notice that the ‘G’ is only found in archaic and modern human ARHGAP11B. Exonic and intronic nucleotide sequences are displayed in upper and lower cases, respectively. Horizontal lines indicate splice donor sites.

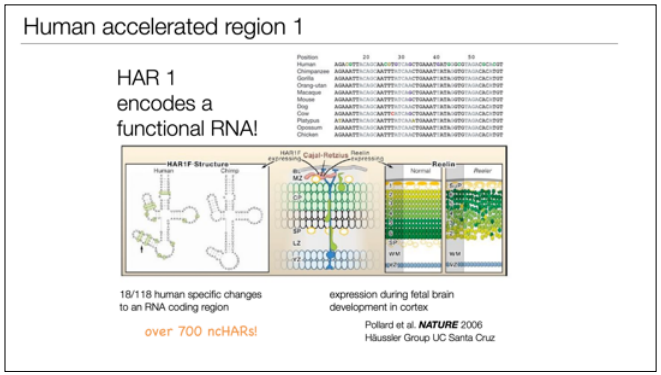

20q13.33 of the HAR1-associated transcripts HAR1F and HAR1R, these micro RNAs associate with the protein Reelin, which is involved in fetal cortex organization.

Endocast = cast of the inside of the braincase

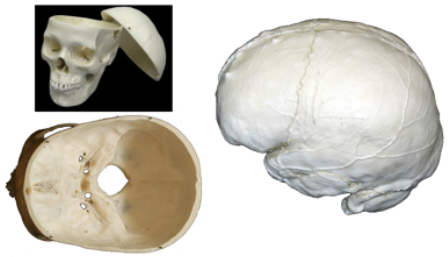

Endocranium

Endocranial cast = endocast

Between the brain and the bone: the meninges

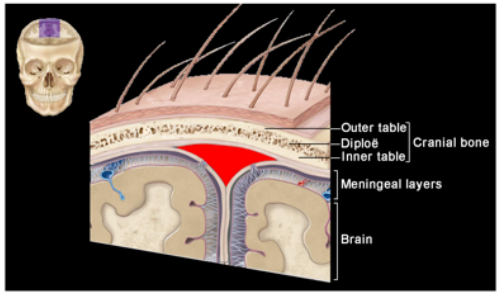

Endocast ≠ brain

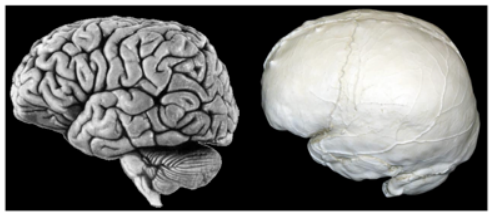

Brain

Endocast

Endocast and Brain Surface

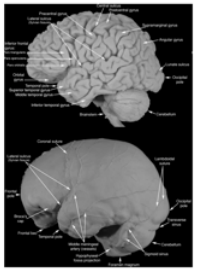

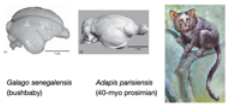

Overall Brain/Endocranial Volume
Relative Size/Shape of Lobes
Convolution Pattern
Asymmetry
Blood Supply Patterns

Holloway et al, 2009

The natural endocasts

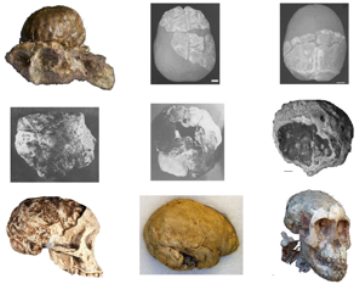

9 natural endocasts of fossil hominins

Australopithecus afarensis child

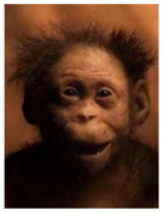

Famous skull with brain enbocast of 3my old A afarensis child Selam (Dikika)

The artificial virtual endocasts from Thibault Bienvenu

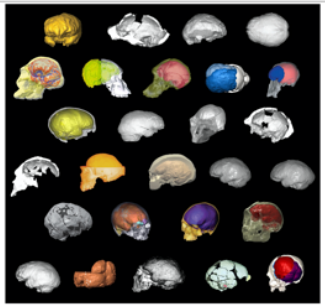

27 virtual endocasts of fossil hominins

Evolution & development: from bones to molecules

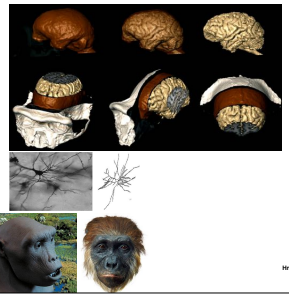

Hrvoj-Mihic, Bienvenue et al., 2013

Brain Anatomy

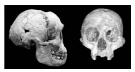

Florea, Indonesia
18,000 ya

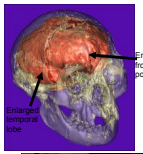

Falk et al., 2005, 2007

Australopithecine Endocasts

Some australopithecine endocasts have distinct features in the frontal and temporal lobes that place them closer to humans than to apes or other extinct hominids

Falk, 2011

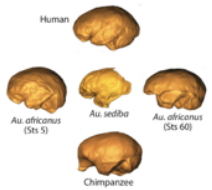

Carlson, et al. , 2011

Orbitofrontal Cortex

Australopithecus sediba
2 my old
420 cc brain volume

Reorganization in orbito-Frontal surface
- Shape
- Relative extent of anterior to posterior regions

The Fossil Record


Bodo
600 ky


Petralona
200-400 ky


Guattari
50 ky

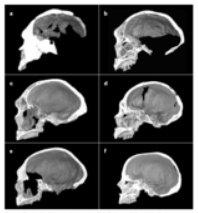


Kabwe
125-300 ky


Atapuerca
300 ky


H. sapiens

Despite differences btn fossil skulls from early hominins, the inner curve of the front of the cranium is nearly identical.

→Shape of the anterior frontal lobe has not changed in recent evolution.

(Bookstein et al., 1999)

Brain Slices

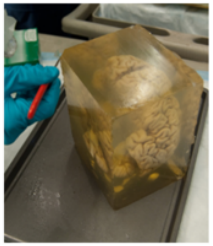

The Brain Observatory, UCSD

QUANTITATIVE, CELLULAR & MOLECULAR ANALYSES

-Cytoarchitecture
-Myeloarchitecture
-Chemoarchitecture
-Gene expression/Molecular:
Geschwind & Rakic, Neuron 2013

HISTOLOGY

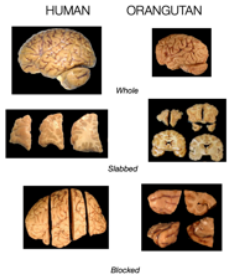

Brain Anatomy

Defining and using Anatomical Boundaries

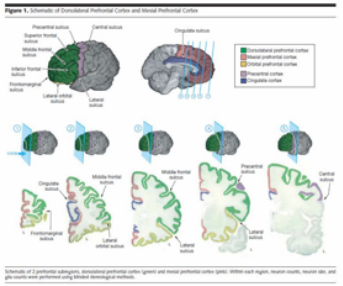

How to slice?

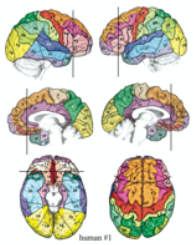

Stereotaxic planes are used with large samples of human brains in imaging.

Such planes cut through cortical territories
→ less informative for questions about volume of cortical regions (eg. frontal cortex or PFC).

Images courtesy of Hanna Damasio

The relative size distribution of areas within the frontal lobe differs between apes & humans

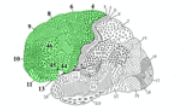

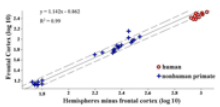

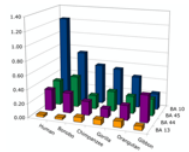

Some frontal cortex areas are relatively larger, others smaller.

Semendeferi et al., 2002
Teffer & Semendeferi 2012

Impulse Control – Orbitofrontal & vmPFC

Phineas Gage

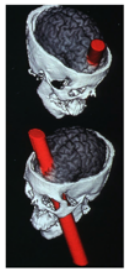

If damaged : changes in the ability to make advantageous decisions in personal, social, and financial domains

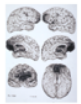

Damage in parts of the frontal lobe in a human brain

Lesion studies
(accidents, disease, strokes)

Imaging Studies
(Functional & Structural)

Barbas, 2007
Heimer & Van Hoesen, 2006
Craig, 2009

Damasio, 1994
Bechara, 2010

Imaging techniques

TABLE 1. Summary of neuroimaging methods

Technique	Example	Purpose	Advantages	Disadvantages
MRI		Anatomical image of gray matter, white matter, and CSF	Can be conducted on anesthetized subjects	Microscopic (cellular) features not visible
DTI		Reconstruction of white matter fiber tracts – imaging anatomical connectivity	Can be conducted on anesthetized subjects	Cannot track individual axons because of limited spatial resolution, cannot discriminate origin from termination of pathways
PET		Imaging brain function (glucose metabolism or blood flow) and receptor density and distribution	^{18}F-FDG PET enables functional imaging without restraint, outside the scanner	Limited temporal resolution (on the order of minutes), involves the administration of radioactive tracers, ^{15}O water PET requires immobilization of awake animals, dependent on access to cyclotron
fMRI		Imaging brain function (blood flow)	Good temporal resolution (seconds), tracer administration not required	Loud, confining environment, requires immobilization of awake animals

Rilling, Yearbook of Phys. Intro 2013

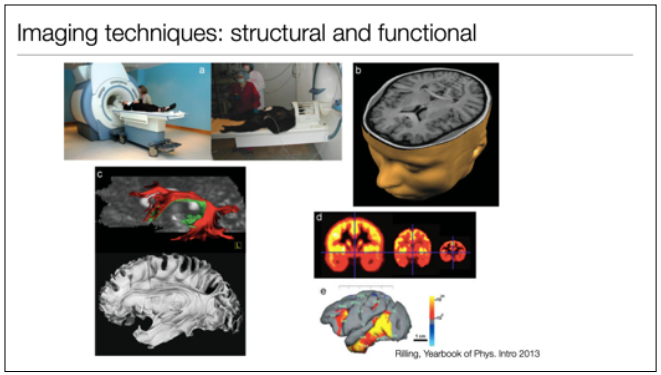

Structural neuroimaging.
(a) MRI scanner with human (left) and chimpanzee (right) subject,
(b) (b) axial section through human T1-weighted MRI scan,
(c) DTI-based reconstruction of the human arcuate fasciculus pathway (top) and postmortem equivalent (bottom),
(d) 18F-FDG PET images from human (left), chimpanzee (middle), and rhesus macaque (right), brighter colors (yellow to white) indicate higher levels of radioactivity and glucose metabolism.
(e) fMRI activations related to object processing in awake rhesus macaque. Colored areas are more active when processing intact compared with scrambled objects. Activation is particularly strong in the ventral temporal cortex, the presumed location of

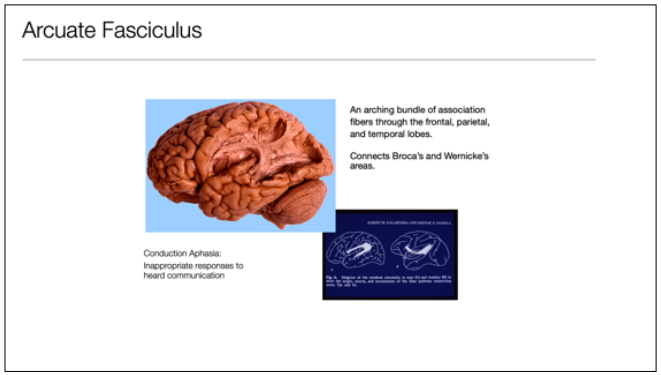

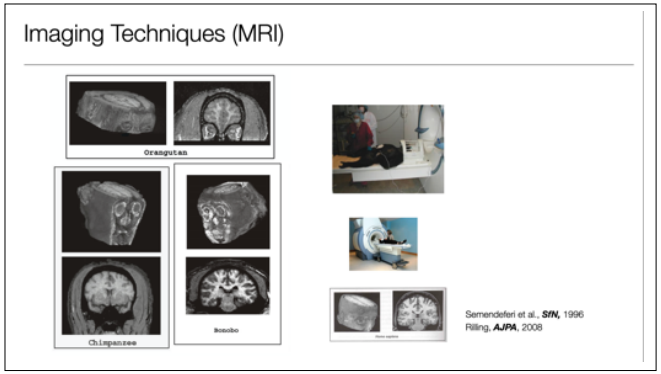

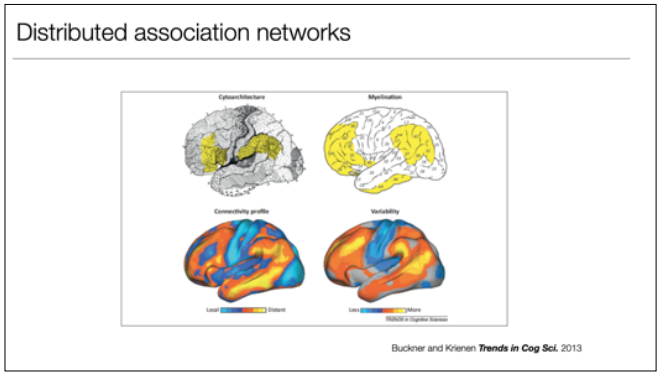

Association cortex matures late and possesses functional properties that are different from sensory regions. Top: Brodmann's (1909) cytoarchitectonic map and Fleschig's (1920) developmental myelination estimates are displayed [28,79]. Numbers for cytoarchitecture arbitrarily label the distinct zones of cortex and have come to be known as Brodmann areas. Regions shaded in yellow are frontal and parietal areas that Brodmann (1909) proposed had no monkey homologs. Myelination numbers designate the relative ordering of developmental myelination, with higher numbers indicating late development. The regions shaded in yellow mature late. Bottom: Functional MRI estimates of organizational properties. Distant connectivity quantifies the relative percentage of strong functional correlations that are distant from the region (e.g., across lobes) versus local correlations. Warmer colors reflect regions that have preferentially long-range functional connectivity. Variability displays regions with the greatest between-subject variation in functional organization estimated by functional connectivity.

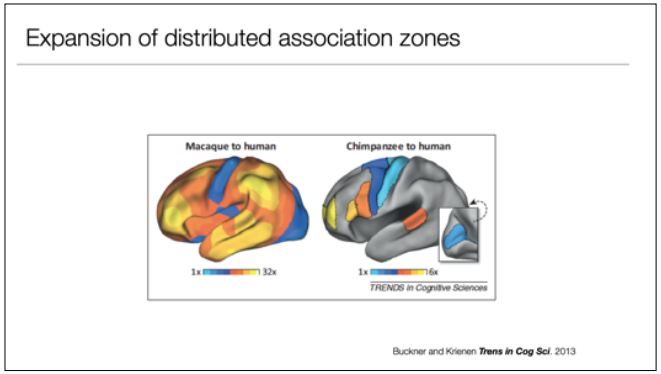

Distributed association zones are disproportionately expanded in humans. Estimated cortical expansion is illustrated for macaque to human and for chimpanzee to human. Colors represent the scaling value required to achieve the size in the human brain. The data are projected onto the left hemisphere cortical surface of the population-average, landmark- and surface-based atlas. For the macaque, a continuous surface estimate of expansion is computed from 23 distributed landmarks. For the chimpanzee expansion plot, area estimates for a limited set of discrete areas are presented from Table 2 in [6]. The primary visual area (V1) is displayed in the inset.

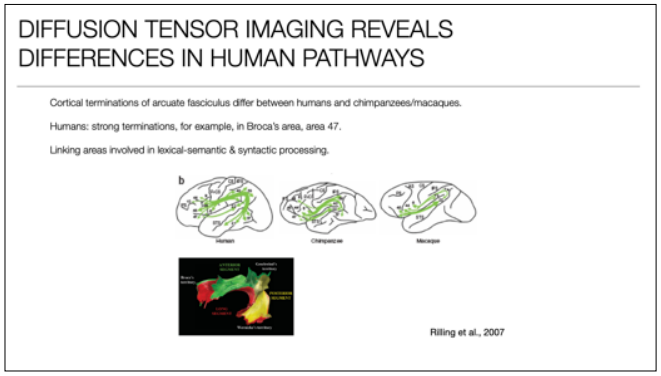

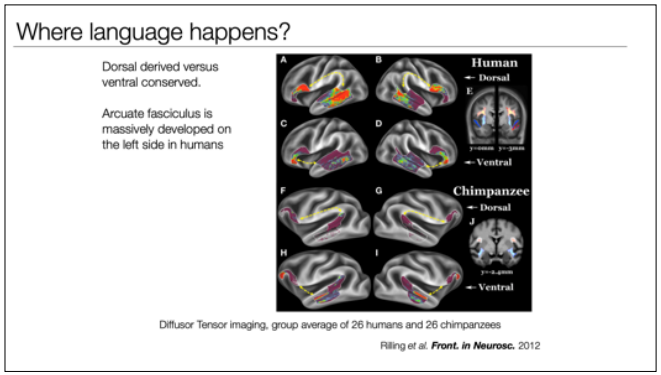

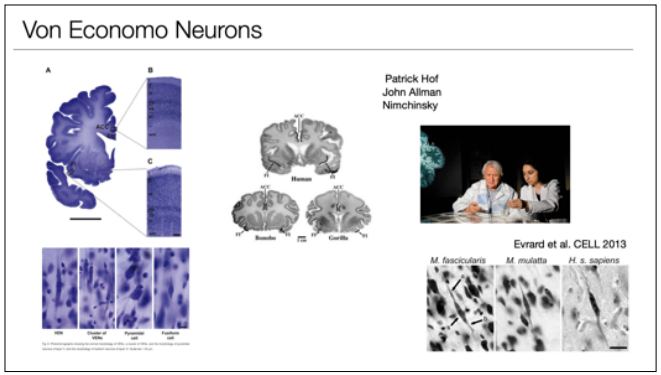

Large conical neurons with particular shapes: VEN Von Economy Neurons

---

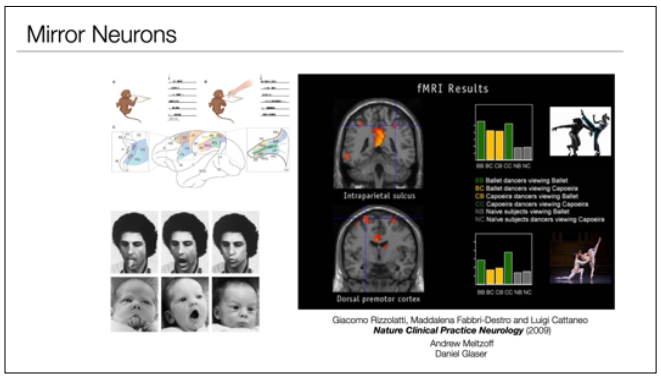

Giacomo Rizzolatti, Maddalena Fabbri-Destro and Luigi Cattaneo Nature Clinical Practice Neurology (2009)
Andrew Meltzoff
Daniel Glaser
Mirror Neurons, how do they look, what is their biochemical signature? No molecular markers.....

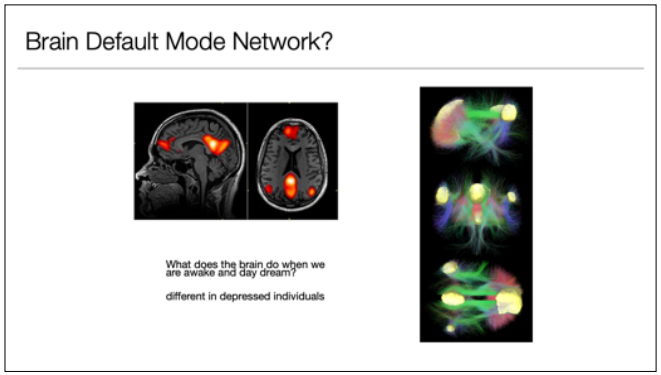

This network is strongly inhibited by LSD and Psilocibin and the inhibition is associated with self reports of “ego-dissolving” sensation. This begs the question about who is watching the “ego” dissolve.

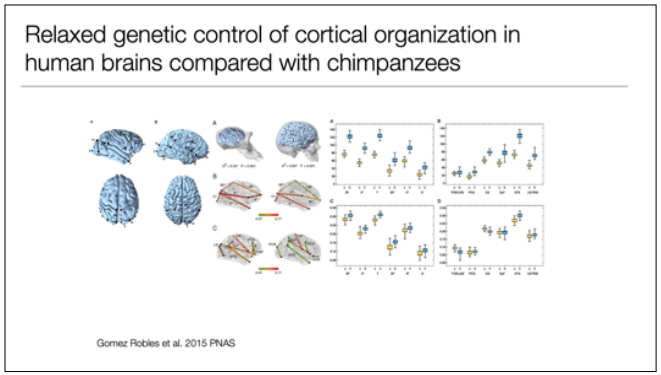

Heritability for brain size and lobe and sulcal dimensions. (A) Heritability for brain size (brain volume including white and gray matter but not ventricular spaces) for chimpanzees (Left) and humans (Right). (B) Heritability for cerebral lobe dimensions in chimpanzees (Left) and humans (Right). IF, inferior frontal length; IP, inferior parietal length; O, occipital length; SF, superior frontal length; SP, superior parietal length; T, temporal length. (C) Heritability for sulcal lengths in chimpanzees (Left) and humans (Right). CS, central sulcus; FOS, fronto-orbital sulcus; LOS, latero-orbital sulcus; LS, lunate sulcus; PCS, precentral sulcus; POS, parieto-occipital sulcus; STS, superior temporal sulcus; SyF, Sylvian fissure. In B and C lobe dimensions and sulci are color-coded according to heritability values as indicated in the color scale bars. Lobe dimensions and sulci marked with an asterisk show significant heritability after a false-discovery rate approach was used to control for multiple comparisons. Detailed heritabilities, SEs, and P values are listed in Tables S3 and S4. In B and C chimpanzee and human brains are not to scale. Boxplots showing variation in linear metrics. Data for chimpanzees (c) are shown in yellow, and data for humans (h) are shown in blue. (A) Variation in original lobe dimensions (in native space). (B) Variation in original sulcal dimensions. In A and B dimensions are provided in millimeters. (C) Variation in lobe dimensions measured in Procrustes-superimposed configurations of landmarks. (D) Variation in sulcal dimensions in Procrustes-superimposed configurations. In C and D linear dimensions were measured after scaling all individuals to a centroid size of 1. In A and C, IF, inferior frontal length; IP, inferior parietal length; O, occipital length; SF, superior frontal length; SP, superior parietal length; T, temporal length. In B and D, CS, central sulcus; FOS, fronto-orbital sulcus; LOS, latero-orbital sulcus; LS, lunate sulcus; PCS, precentral sulcus; POS, parieto-occipital sulcus; STS, superior temporal sulcus; SyF, Sylvian fissure. Anatomically homologous landmarks used in this study. (A) Anatomically homologous landmarks in chimpanzee brains in lateral view (Upper) and dorsal view (Lower). (B) Anatomically homologous landmarks in a representative human brain in

lateral view (Upper) and dorsal view (Lower).

Neuronal migrations in the neonatal brain

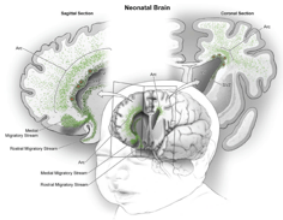

during first 7 months of life, neurons migrate into the anterior cingulate cortex

Paredes *et al.* ***Science*** 2016

Relatively larger and smaller

Orbitofrontal cortex is larger in humans, dorsal is smaller

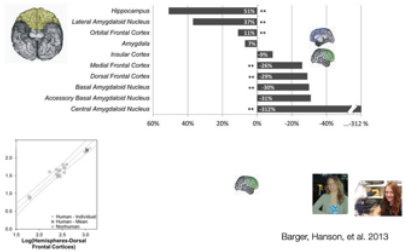

Barger, Hanson, et al. 2013

Neuropil: space around neurons

Human brains have decreased cell body density and more space available for connections.

Zilles et al., 1986

The human brain has differentially increased neuropil space in the layer III of PFC.

Semendeferi et al., 2001

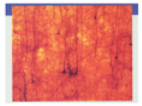

Neuropil is the amount of space around cell bodies available for connections (dendritic arbors, axons, glia, vasculature)

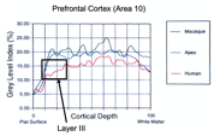

Brain Anatomy

Increased Spacing between Neuronal Bodies

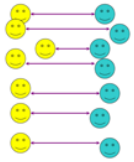

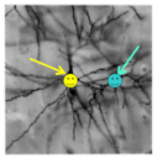

Differences in branching morphology of neurons?

Jacobs et al., 2009
Elston et al., 2005
Petanjek et al., 2008
De Felipe, 2005
Bianchi 2013

Branching Patterns

Branching of pyramidal neurons in the dorsolateral PFC increases during development in humans (and non human primates)

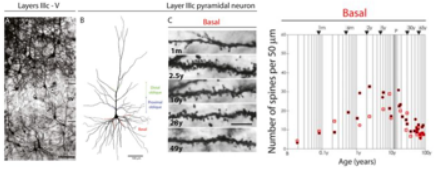

Petanjek et al., 2011

DENDRITIC COMPLEXITY

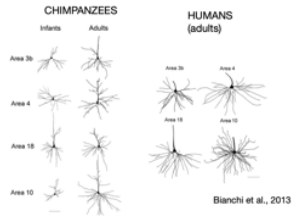

Bianchi et al., 2013

Chimps: Greater dendritic complexity in PFC than other areas.
Complexity increases in early development
Humans: Longer and more branched across areas

SPACING OF CELLS

Is the spacing of the neurons and thus the size of minicolumns predicted by overall brain size? No

Is the spacing the same among cortical areas within each brain? No

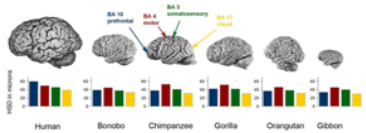

Humans have more space than apes between neuronal bodies in areas of the Prefrontal Cortex but not as much in other parts of the brain

Semendeferi/Teffer *et al*, ***Cerebral Cortex*** 2011

Human frontal cortex has a higher ratio of glia to neurons

- Glial cells regulate the rate of glucose uptake, and thus the flux of energy, to neurons.
- Increased number of glia relates to energetic costs of maintaining larger dendritic arbors and long range projecting axons in the human brain.

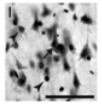

Nissl staining of neurons and glia in layer II/III in *Pongo pygmaeus* prefrontal Cortex.

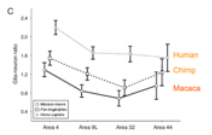

Sherwood et al., 2006

Neuron numbers in lateral nucleus of amygdala stand out in humans

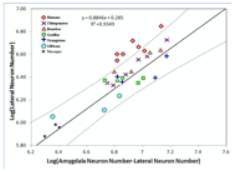

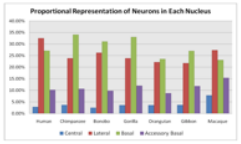

- The amygdala has a unique organization in humans
- The lateral nucleus is the largest component of the basolateral division in humans
- Apes have the largest basal nucleus

Barger et al, JCN 2012

Lateral nucleus of Amygdala

Lateral nucleus is highly interconnected with the temporal lobe.

Helen Barbas; Lisa Stefanacci

Semendeferi & Damasio, 2000
Rilling & Religman, 2001

Barger et al., 2007, 2012

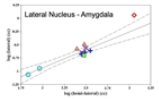

Lateral nucleus larger in humans

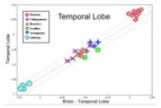

Temporal lobe larger in humans

Mutations in individual Neurons: Polyclonal Architecture!!

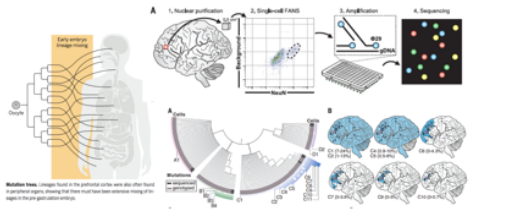

Lodato et al., ***SCIENCE*** 2015
Chris Walsh Group Harvard

COVER Illustration of projection neurons from the human cerebral cortex, with nuclei colored to reflect distinct sets of somatic DNA mutations. When a mutation occurs in a dividing cell, it marks all of the cell's descendants. Identification of clones marked by mutation enables reconstruction of human brain development. Because developmental defects lie at the heart of many neurological diseases, understanding development is a primary goal of neuroscience.

Somatic L1 (retrotransposon) Associated Variants

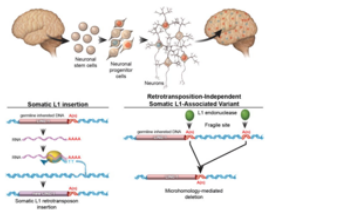

Erwin *et al.*, ***Nat Neuroscience*** 2016
Rusty Gage Group at SALK

For somatic L1 insertions, a germline-inherited LINE-1 sequence is transcribed into RNA. The L1 endonuclease and reverse transcriptase protein nicks the genomic DNA and reverse transcribes the L1 RNA, resulting in the insertion of a new copy of Line-1 sequence. For retrotransposition-independent SLAVs, L1 endonuclease preferentially cuts a a germline-inherited LINE-1 sequence and recombination with a downstream A microsatellite results in a microhomology-mediated deletion. The A microsatellite regions may be nicked by the L1 endonuclease or a fragile site within the genome of neural progenitor cell.

Brain expansion over time

Driven by culture and/or driving culture?

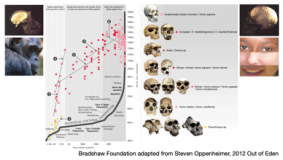

Bradshaw Foundation adapted from Steven Oppenheimer, 2012 Out of Eden

---

Summary Brain Evolution

- Brain changes range from the macro to the nano.
- Tripling of absolute brain size in the last 3 million years.
- Fossil endocasts and virtual endocasts shed some light on gross dimensions over that past 6 my.
- Imaging techniques allow comparative neuroanatomy in live hominids.
- Human brains grow for longer and at sustained rates in utero and after birth.
- Delayed maturation and expression of genes, synaptogenesis and myelinization in humans.
- Human neocortex is not larger than expected for a primate our size.
- Connectivity has changed, e.g. intra-hemispheric is higher in humans, arcuate fasciculus is much expanded.
- Neuron morphology, numbers and distribution vary in several regions of the human brain.
- Subcortical areas especially the amygdala (social brain) has undergone human specific changes.
- Cell-type specific changes: VEN and mirror neurons?
- Novel genes and gene variants are involved.